52nd AIAA/ASME/ASCE/AHS/ASC Structures, Structural Dynamics and Materials Conference
 19th
4 - 7 April 2011, Denver, Colorado

AIAA 2011-2168

Analysis of slender, thin walled, composite made structures with refined 1D theories

E. Carrera*

Department of Aeronautic and Space Engineering, Politecnico di Torino, 10129, Italy

M. Petrolo†

Department of Aeronautic and Space Engineering, Politecnico di Torino, 10129, Italy, and Institut Jean Le Rond d'Alembert, UMR7190 CNRS, Paris06, 75252 Paris, France

Downloaded by UNIVERSITY OF MICHIGAN on March 7, 2014 | http://arc.aiaa.org | DOI: 10.2514/6.2011-2168

A novel refined 1D model for the analysis of thin walled composite structures is presented in this paper. The proposed model is embedded in the framework of the Carrera Unified Formulation, CUF, which is focused on the development of higher-order beam/plate/shell models. The displacement field above the structure cross-section is modeled by means of polynomial expansions whose form and order is arbitrary, this means that any-order 1D models are obtainable in a unified and hierarchical manner. Taylor- and Lagrange-type expansions are adopted. The former leads to an Equivalent Single Layer description of the structure where the refinement of the model is obtained by increasing the order of the polynomial expansion. The latter permits us to obtain a Layer-Wise description with only displacement variables and the possibility of locally refining the model by assembling an arbitrary number of Lagrange polynomial sets. A finite element formulation is used to be able to deal with different loading and boundary conditions. A number of structural problems concerning composite made structures is presented and the results are compared with those from refined plate finite elements. The analyses carried out highlight that the present beam formulation is able to: 1. detect the plate solution; 2. keep the computational cost low; 3. analyze problems that can be usually addressed by 2D or 3D models only (e.g. laterally constrained structures or open thin walled cross-section beams).

I. Introduction

Most of the aerospace structures appear as slender and thin walled. Examples are aircraft wings and fuselages, missiles, helicopter blades, propellers, and wind energy turbines. Most of these structures are made of advanced, anisotropic, multilayered composite materials. Their rational design and analysis is a fundamental task for the structural analysts; an accurate evaluation of their static, dynamic, buckling, aeroelastic, and fatigue responses requires adequate models. The complete response calculation is a quite complex task and, in some cases, it would demand the solution of nonlinear problems. The need of accurate and, at the same time, computationally efficient structural models is the key-point for a rational design and analysis of these complex structures.

Various structural models are known. Beam (1D) analyses are preferred but plate/shell (2D) and tree-dimensional (3D) solutions are used in some cases to provide reasonable results. Computational methods are implemented to provide solutions for complex geometries, loading and boundary conditions. These methods, such as the Finite Element Method FEM, to which the attention is focused in this work, lead to increasing computational costs whenever a 3D or 2D analysis is employed. Plate/shell and solid FE element formulations can be efficiently used if and only if some aspect ratio constraints are fulfilled. The aspect ratios of the plate/shell/solid elements employed should not exceed some fixed values (less than 10[1–3]). This

*Professor, Department of Aeronautic and Space Engineering, Politecnico di Torino, Corso Duca degli Abruzzi, 24, 10129 Torino, Italy, erasmo.carrera@polito.it

†PhD Student, Department of Aeronautic and Space Engineering, Politecnico di Torino, Corso Duca degli Abruzzi, 24, 10129 Torino, Italy, marco.petrolo@polito.it., and Institut Jean Le Rond d'Alembert, UMR7190 CNRS, Paris06, Case 162, Tour 55-65, 4, Place Jussieu, 75252 Paris, France.

Copyright © 2011 by the American Institute of Aeronautics and Astronautics, Inc. All rights reserved.

constraint can lead to very high computational costs since the number of the elements employed can increase very much.

The adoption of refined 1D theories can permit us to avoid the more cumbersome shell or solid models. Excellent works on this issue are those by Kapania and Raciti[4,5] and Yu et alii.[6,7] In a series of recent works,[8–13, 13–16] the authors have clearly shown that refined 1D models can be used instead of the 2D and 3D ones to describe shell type behaviors and localized three-dimensional effects. One of the main advantage of an 1D formulation is that it does not have aspect ratio constraints, therefore, computationally efficient models of slender structures can be built with acceptable costs.

Refined 1D models are built on the basis of the Carrera Unified Formulation (CUF) that was originally proposed by the first author for laminated plates and shells,[17,18] and recently extended to beams.[8,9] The refined beam theories and the related finite elements are obtained by exploiting an $any-order$, N, expansion of the displacement variables over the structure section, these models can be easily implemented since the governing equations as well as the finite element matrices are written in terms of a few fundamental nuclei whose form does not vary by changing N, the base functions (i.e. the polynomials that are used to express the displacement variables over the beam section), or the number of the nodes along the structure axis.

The refined 1D model based on CUF is in this paper extended to consider slender bodies made of laminated structures based on anisotropic composite materials. The Lagrange polynomials are conveniently used to simulate laminated layers and interfaces.

Downloaded by UNIVERSITY OF MICHIGAN on March 7, 2014 | http://arc.aiaa.org | DOI: 10.2514/6.2011-2168

II. Advanced 1D Theories

In the framework of the Carrera Unified Formulation (CUF), the displacement field is the expansion of generic functions, F_τ:

$$\mathbf{u}(x,y,z) = F_\tau(x,z)\mathbf{u}_\tau(z), \qquad \tau = 1,2,....,M \tag{1}$$

where F_τ vary above the cross-section. $\mathbf{u}_\tau$ is the displacement vector and M stands for the number of terms of the expansion. According to the Einstein notation, the repeated subscript, τ, indicates summation. Fig. 1 shows the coordinate reference system adopted. Taylor-type expansions have been exploited in previous works

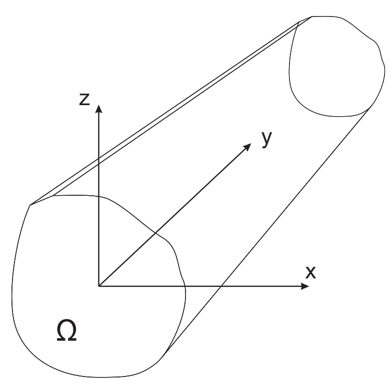

Figure 1. Coordinate frame of the structure.

by Carrera and co-workers.[8–15] The Euler-Bernoulli (EBBM) and Timoshenko (TBM) classical theories are derived from the linear Taylor-type expansion. Lagrange polynomial based models have been recently introduced by Carrera and Petrolo.[19] Nine-point, L9, polynomials defined on quadrilateral domains are adopted here. The isoparametric formulation is exploited and the interpolation functions are given by:

$$\begin{aligned}
&F_\tau = \tfrac{1}{4}(r^2 + r\, r_\tau)(s^2 + s\, s_\tau) \qquad \tau = 1,3,5,7 \\
&F_\tau = \tfrac{1}{2}s_\tau^2(s^2 - s\, s_\tau)(1-r^2) + \tfrac{1}{2}r_\tau^2(r^2 - r\, r_\tau)(1-s^2) \\
&\qquad \tau = 2,4,6,8 \\
&F_\tau = (1-r^2)(1-s^2) \qquad \tau = 9
\end{aligned} \tag{2}$$

Where r and s from -1 to $+1$. Fig. 2 shows the point locations and Table 1 reports the point natural coordinates. The displacement field given by an L9 element is:

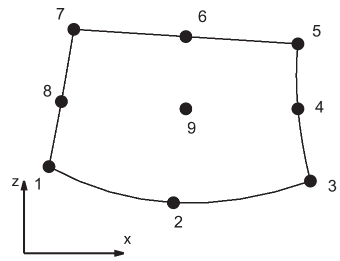

Figure 2. L9 cross-Section element points.

Table 1. L9 cross-section element point natural coordinates.

Point	r_τ	s_τ
1	-1	-1
2	0	-1
3	1	-1
4	1	0
5	1	1
6	0	1
7	-1	1
8	-1	0
9	0	0

$$\begin{aligned} u_x &= F_1\, u_{x_1} + F_2\, u_{x_2} + F_3\, u_{x_3} + F_4\, u_{x_4} + F_5\, u_{x_5} + F_6\, u_{x_6} + F_7\, u_{x_7} + F_8\, u_{x_8} + F_9\, u_{x_9} \\ u_y &= F_1\, u_{y_1} + F_2\, u_{y_2} + F_3\, u_{y_3} + F_4\, u_{y_4} + F_5\, u_{y_5} + F_6\, u_{y_6} + F_7\, u_{y_7} + F_8\, u_{y_8} + F_9\, u_{y_9} \\ u_z &= F_1\, u_{z_1} + F_2\, u_{z_2} + F_3\, u_{z_3} + F_4\, u_{z_4} + F_5\, u_{z_5} + F_6\, u_{z_6} + F_7\, u_{z_7} + F_8\, u_{z_8} + F_9\, u_{z_9} \end{aligned} \tag{3}$$

Where $u_{x_1}, ..., u_{z_9}$ are the displacement variables of the problem and they represent the translational displacement components of each of the nine points of the L9 element. The cross-section can be discretized by means of several L-elements. Fig. 3 shows the assembly of 2 L9 which share a common edge and three points.

A. Finite Element Formulation

The discretization along the structure axis is conducted via a classical finite element approach. The displacement vector is given by:

$$\mathbf{u}_\tau = N_i F_\tau \mathbf{q}_{\tau i} \tag{4}$$

Where N_i stands for the shape functions and $\mathbf{q}_{\tau i}$ for the nodal displacement vector:

$$\mathbf{q}_{\tau i} = \left\{ \begin{array}{ccc} q_{u_{x_{\tau i}}} & q_{u_{y_{\tau i}}} & q_{u_{z_{\tau i}}} \end{array} \right\}^T \tag{5}$$

For the sake of brevity, the shape functions are not reported here. They can be found in many books, for instance in.[20] Elements with four nodes (B4) are here formulated, that is, a cubic approximation along the y axis is adopted. It has to be highlighted that the adopted cross-section displacement field model defines the 1D model. Further refinements can be obtained by adding cross-section elements, in this case the model will be defined by the number of cross-section elements used. The choice of the cross-section discretization (i. e. the choice of the type, the number and the distribution of cross-section elements) is completely independent of the choice of the finite element to be used along the structure axis.

Downloaded by UNIVERSITY OF MICHIGAN on March 7, 2014 | http://arc.aiaa.org | DOI: 10.2514/6.2011-2168

Downloaded by UNIVERSITY OF MICHIGAN on March 7, 2014 | http://arc.aiaa.org | DOI: 10.2514/6.2011-2168

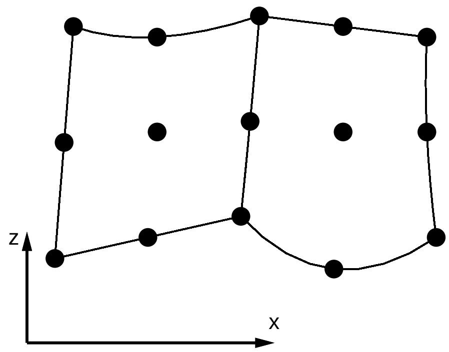

Figure 3. Two assembled L9 elements.

Finite element matrices , which are consistent with the model, are obtained via the Principle of Virtual Displacements in the form of the *fundamental nuclei*. A component of the 3×3 stiffness matrix nucleus is:

$$\begin{aligned} K_{xx}^{ij\tau s} = & \tilde{C}_{22} \int_{\Omega} F_{\tau,x} F_{s,x} d\Omega \int_l N_i N_j dy + \tilde{C}_{44} \int_{\Omega} F_{\tau,z} F_{s,z} d\Omega \int_l N_i N_j dy + \\ & \tilde{C}_{66} \int_{\Omega} F_{\tau} F_s d\Omega \int_l N_{i,y} N_{j,y} dy + \tilde{C}_{26} \int_{\Omega} F_{\tau,x} F_s d\Omega \int_l N_i N_{j,y} dy + \\ & \tilde{C}_{26} \int_{\Omega} F_{\tau} F_{s,x} d\Omega \int_l N_{i,y} N_j dy \end{aligned} \tag{6}$$

It should be noted that no assumptions on the approximation order have been made. It is therefore possible to obtain refined beam models without changing the formal expression of the nucleus components. This is the key-point of CUF which permits, with only nine FORTRAN statements, to implement any-order 1D theories. The shear locking is corrected through the selective integration (see[20]). The line and surface integral computation is numerically performed by means of the Gauss method. The assembly procedure of the Lagrange-type elements is analogous to the one followed in the case of 2D elements. The procedure keypoints are briefly listed:

1. The fundamental nucleus is exploited to compute the stiffness matrix of each structural node of each cross-section element. If an L9 element is considered, this matrix will have 27×27 terms.

2. The stiffness matrix of the structural node is then assembled by considering all the cross-section elements and exploiting their connectivity.

3. The stiffness matrix of each beam element is computed and assembled in the global stiffness matrix.

III. Numerical Results

Numerical examples are here illustrated in order to highlight the enhanced capabilities of the present 1D formulation. The attention is paid to the analysis of thin walled structures and a longeron model.

A. Cross-Ply and Sandwich Plates

A thin composite plate is first considered, its geometry is shown in Fig. 4 . Its length, L, is equal to 1 [m], the width, b, is equal to 0.1 [m], and the thickness, t, is equal to 0.01 [m]. Both ends are clamped. An orthotropic material is adopted with E_L as equal as 40 [GPa], E_T and E_z equal to 4 [GPa], ν equal to 0.25, and G equal to 1 [GPa]. The plate is cross-ply, 0/90/0, each layer thickness is equal to $t/3$. Three point loads, F_z, are applied at the mid-spanwise bottom side with $x = -b/2, 0$, and $b/2$. A fourth-order layer-wise plate finite element model, LD4, is used for comparison purposes, this model has been obtained by means of the MUL² developed by the authors.[21]

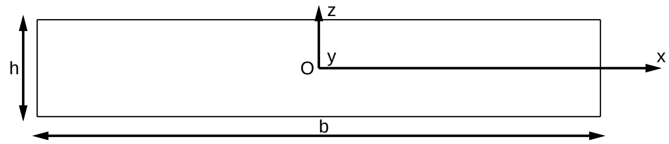

Figure 4. Rectangular cross-section.

Table 2 shows the center point vertical displacement, u_z, at $y = L/2$. Classical models, EBBM and TBM, are considered together with a fourth-order, $N = 4$, Taylor beam model, and two L9 Lagrange models. The number of degrees of freedom of each model is shown in the second column. Fig.s 5 and 6 show two stress distributions along the thickness direction at $x, y = 0$.

Downloaded by UNIVERSITY OF MICHIGAN on March 7, 2014 | http://arc.aiaa.org | DOI: 10.2514/6.2011-2168

Table 2. Vertical displacement, u_z, of the cross-section center point at $y = L/2$.

	DOF's	$u_z \times 10^5$ [m]
	1D - Taylor	
EBBM	305	-4.415
TBM	1395	-4.420
$N = 4$	2745	-4.909
	1D - Lagrange	
$3\times$ L9	3843	-4.909
$6\times$ L9	6405	-4.968
	Plate	
Plate	9945	-5.023

A three-layer sandwich plate is now considered, see Fig. 7. The outer layers are made of an isotropic material ($E = 75$ GPa, $\nu = 0.33$) and are 0.001 m thick. The inner layer is made of a isotropic foam ($E = 3$ MPa, $\nu = 0.25$) and is 0.008 m thick. The width, b, of the plate is equal to 0.01 m; the length, L, is equal to 1 m. A set of five point loads is placed on the top surface at $L/2$. The plate tips are both clamped. These results suggest what follows.

Table 3. Vertical displacement, u_z, and axial stress σ_{yy} of the sandwich plate.

9 L9	Plate
$u_z \times 10^{+3}$ m	
-0.967	-1.018
$\sigma_{yy} \times 10^{-6}$ Pa	
$+3.626$	$+3.329$

1. The proper detection of the displacement field is possible by means of refined beam theories only. The Lagrange based models are particularly effective in detecting the vertical component of the displacement vector, the solution is greatly improved by the adoption of finer cross-section Lagrange discretizations.

2. The computation of the stress distribution is also positively affected by the use of refined models.

3. The computational cost of the present beam formulation is lower than the one requested by the plate model.

B. Composite Longeron

One of the most important capabilities of the present 1D formulation is given by the possibility of deling with solid-like BCs. Classical beam models allow us to impose constraint only above the cross-section, Lagrange

Downloaded by UNIVERSITY OF MICHIGAN on March 7, 2014 | http://arc.aiaa.org | DOI: 10.2514/6.2011-2168

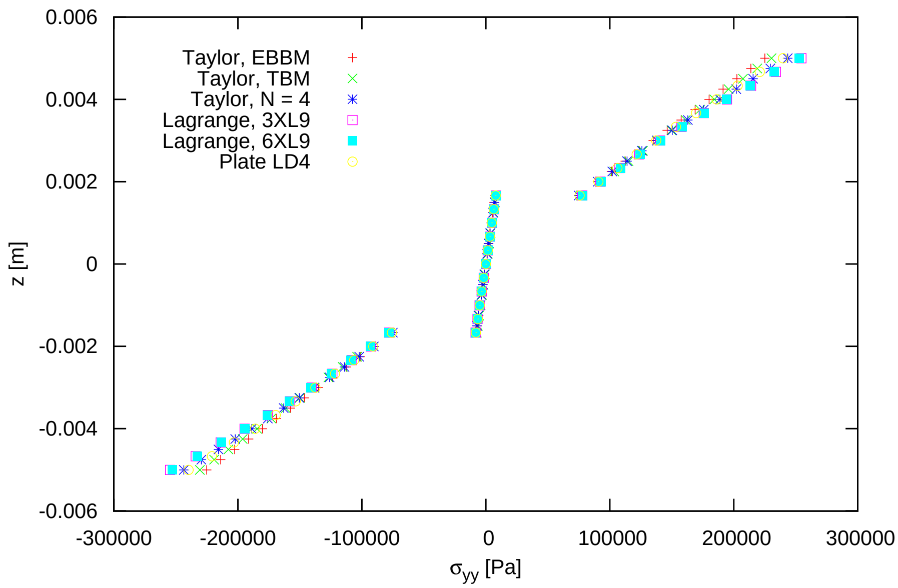

Figure 5. Axial stress, σ_{yy}, distribution at $x = 0$, $y = 0$.

CUF 1D models overcome this limitation since each Lagrange point of the structure can be constrained singularly. Fig. 8 shows a graphic description of what is meant for solid-like BCs.
A longeron model is here considered and it is shown in Fig. 9; Table 4 presents the geometrical data of the structure. The unidirectional layers, UD, are made of an orthotropic material with the following characteristics: the Young modulus along the longitudinal axis, E_L, is equal to 40 GPa, and those along the transverse directions are equal to 4 GPa. The Poisson ratio, ν, is equal to 0.25 , and the shear modulus, G, is equal to 1 GPa; the same Poisson and shear modulus values are used in all directions. The foam core is modeled with an isotropic material with E equal to 50 MPa, and ν equal to 0.25. Two unitary point loads are applied and the bottom UD flanges of the free tips are clamped. Results are obtained by considering a Lagrange 1D CUF model having 12 L9 elements above the cross-section. Fig. 10 shows the deformed 3D

	m
L	1.000
a	0.100
b	0.044
c	0.040
h	0.100
t	0.080

Table 4. Composite longeron cross-section dimensions.

configuration of the structure, whereas the free tip deformed cross-section is given in Fig. 11. The vertical and horizontal components of the displacement vector of the loaded point are shown in Table 5. The analysis of the results suggests what follows.

- CUF 1D models are particularly indicated to detect in-plane distortions of the cross-section.
- 3D displacement fields can be obtained easily.

Downloaded by UNIVERSITY OF MICHIGAN on March 7, 2014 | http://arc.aiaa.org | DOI: 10.2514/6.2011-2168

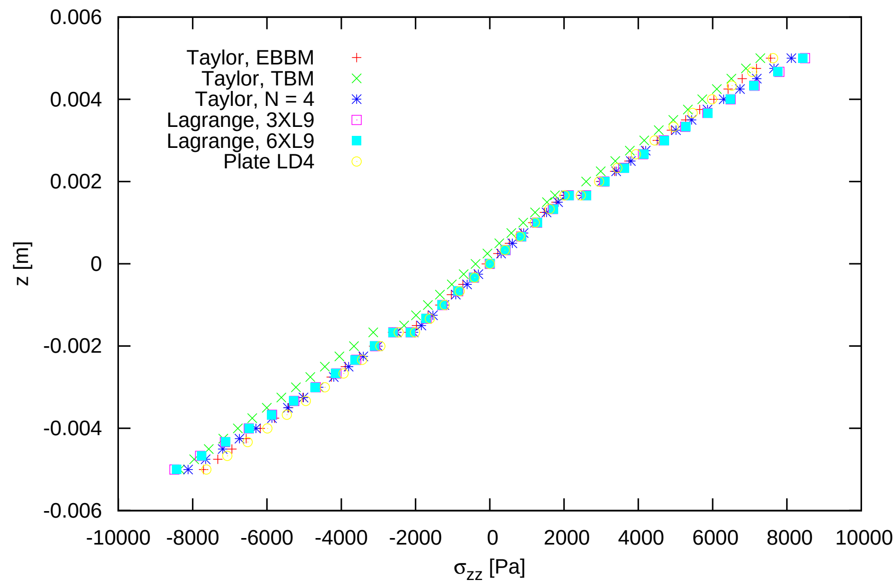

Figure 6. Normal shear stress, σ_{zz}, distribution at $x = b/2$, $y = 0$.

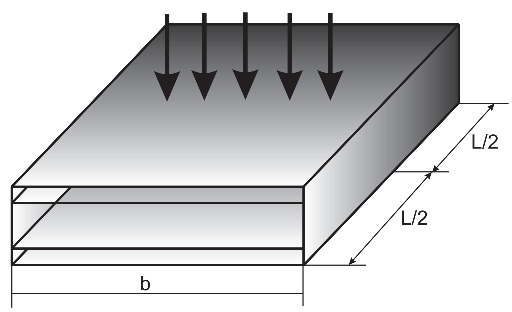

Figure 7. Sandwich Plate.

- The Lagrange models are able to model arbitrary BCs.

C. Cracked Cross-Section Plate

The last assessment of this paper deals with a cracked plate as shown in Fig. 12. The length of the structure is equal to 1 m, widths, b_1 and b_2, are equal to 0.056 and 0.044 m, respectively. The plate is 0.02 m thick. Six unitary point loads are applied and the vertical edges of the left side are clamped at $y = 0$, $L/2$, and L. The same orthotropic material used above is here adopted. Results are obtained by using a 4 L9 CUF 1D model. The displacement components of one of the loaded point of the free tip are presented in Table 6; the deformed configurations are given in Fig.s 13 and 14; a stress distribution above the free-tip is shown in Fig. 15.

It can be stated that:

- the present 1D formulation is able to describe the mechanical behavior of thin walled structures having open cross-sections.
- It is confirmed the capability offered by present models to detect 3D stress fields.

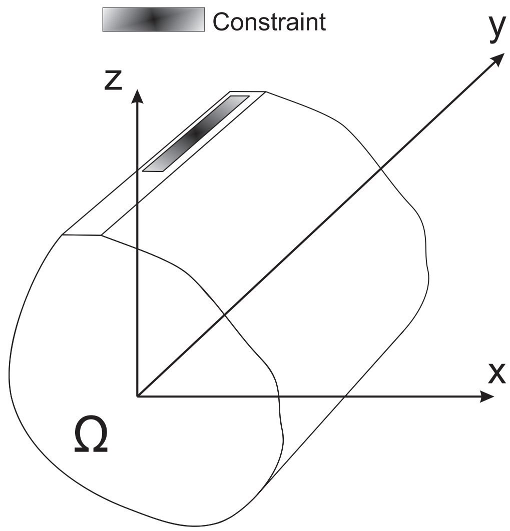

Figure 8. Solid-like BCs.

Table 5. Vertical and horizontal displacements, u_z and u_x, of the loaded point of the longeron.

$u_z \times 10^{+6}$ m	$+5.631$
$u_x \times 10^{+6}$ m	-1.294

IV. Conclusions

This paper has presented a novel 1D refined formulation for composite structures. The proposed formulation is embedded in the framework of the Carrera Unified Formulation, CUF, which has been developed over the last decade for plate/shell/beam models. CUF 1D models are based on two classes of displacement filed expansions over the cross-section: Taylor- and Lagrange-based models. Particular attention has been paid to the former one in this paper. A finite element formulation has been exploited to be able to deal with any type of geometries and loading conditions. Several numerical examples have been carried out on thin walled structures under arbitrary boundary conditions. It can be concluded that:

- the present 1D formulation overcomes the typical limitations of classical beam theories, such as:in-plane distortions, warping, shear effects.
- CUF 1D Lagrange models are particularly indicated to deal with arbitrary BCs and open cross-sections.
- The 1D formulation advantages in terms of computational costs and implementation issues are significative if compared to plate, shell, and solid models.

Future works could deal with non-linear analyses, multiscale problems, and fluid-structure-interaction models.

Acknowledgments

The Regione Piemonte project MICROCOST is gratefully acknowledged for the financial support.

Downloaded by UNIVERSITY OF MICHIGAN on March 7, 2014 | http://arc.aiaa.org | DOI: 10.2514/6.2011-2168

Downloaded by UNIVERSITY OF MICHIGAN on March 7, 2014 | http://arc.aiaa.org | DOI: 10.2514/6.2011-2168

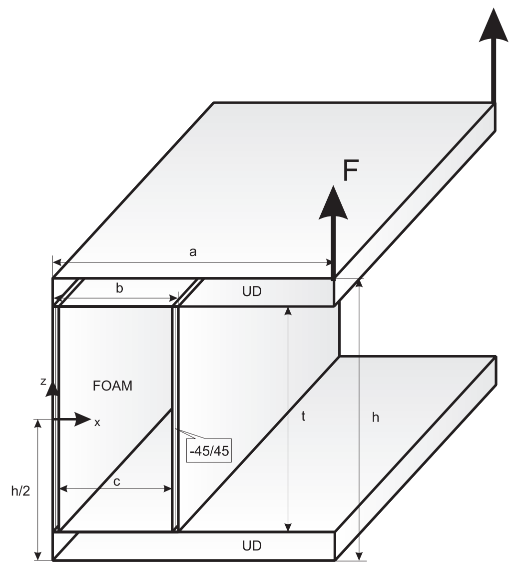

Figure 9. Composite longeron with the bottom flange being clamped.

Table 6. Vertical and horizontal displacements, u_z and u_x, of the loaded point of the cracked plate.

$u_z \times 10^{+6}$ m	-2.730
$u_x \times 10^{+6}$ m	$+4.396$

Downloaded by UNIVERSITY OF MICHIGAN on March 7, 2014 | http://arc.aiaa.org | DOI: 10.2514/6.2011-2168

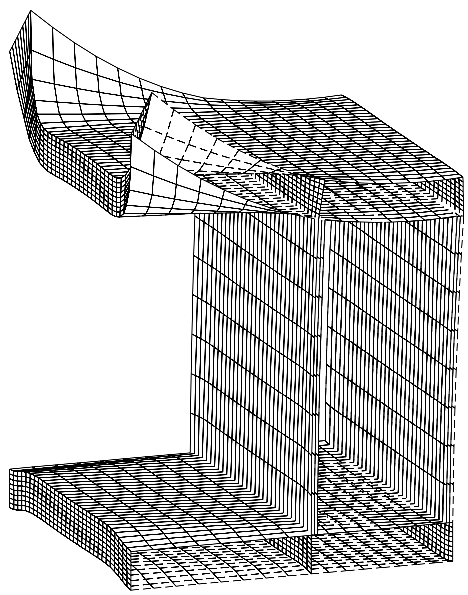

Figure 10. 3D deformed configuration of the longeron.

Downloaded by UNIVERSITY OF MICHIGAN on March 7, 2014 | http://arc.aiaa.org | DOI: 10.2514/6.2011-2168

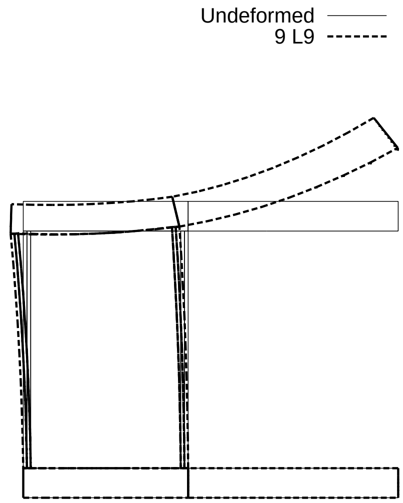

Figure 11. Deformed cross-section of the longeron.

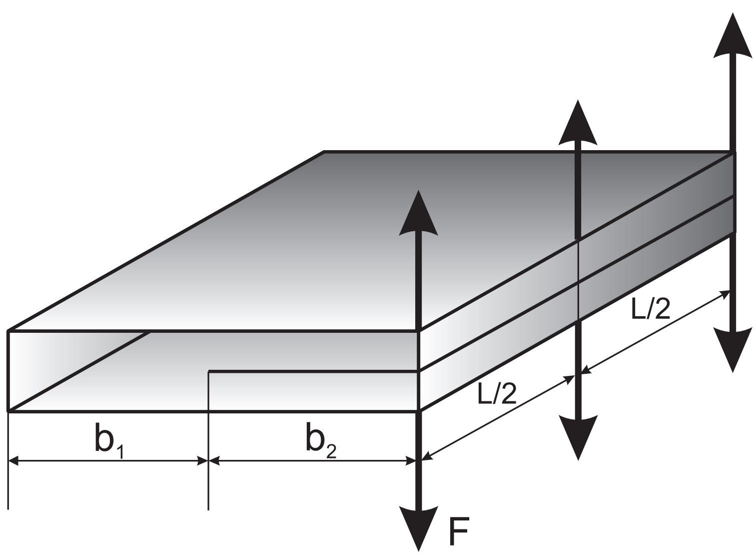

Figure 12. Orthotropic plate with a spanwise crack

Downloaded by UNIVERSITY OF MICHIGAN on March 7, 2014 | http://arc.aiaa.org | DOI: 10.2514/6.2011-2168

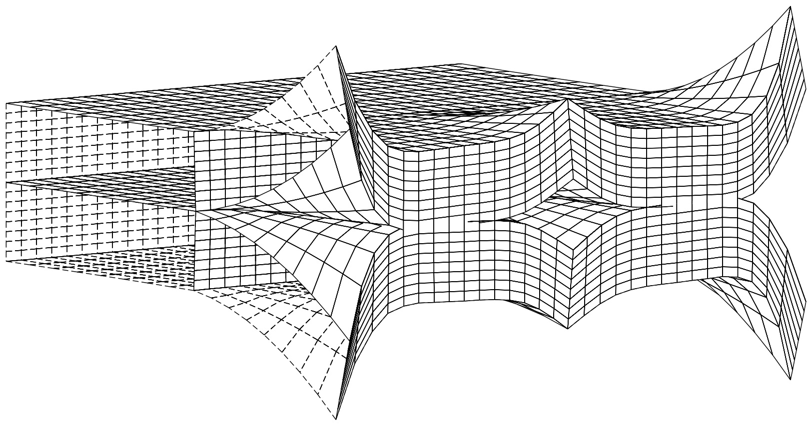

Figure 13. 3D deformed configuration of the orthotropic plate.

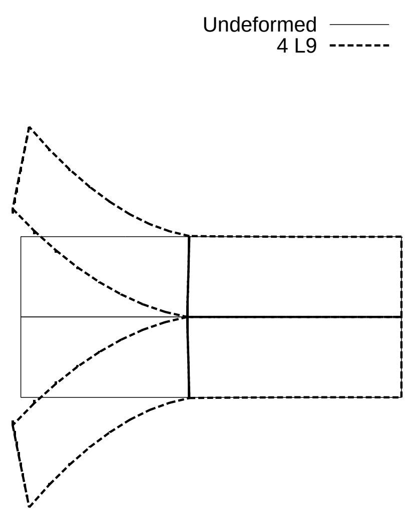

Figure 14. Deformed cross-section of the orthotropic plate.

Downloaded by UNIVERSITY OF MICHIGAN on March 7, 2014 | http://arc.aiaa.org | DOI: 10.2514/6.2011-2168

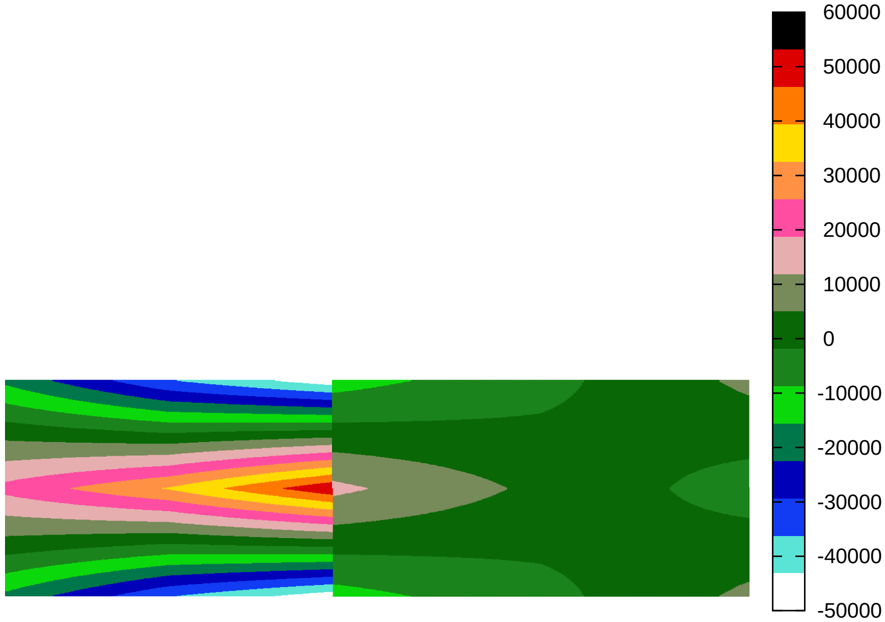

Figure 15. $\sigma_{xx}-$**distribution above the cross-section of the orthotropic plate, Pa.**

References

[1] *MSC Nastran User's Guide*.

[2] *Abaqus User's Guide*.

[3] *Ansys User's Guide*.

[4] Kapania, K. and Raciti, S., "Recent Advances in Analysis of Laminated Beams and Plates, Part I: Shear Effects and Buckling," *AIAA Journal*, Vol. 27, No. 7, 1989, pp. 923–935.

[5] Kapania, K. and Raciti, S., "Recent Advances in Analysis of Laminated Beams and Plates, Part II: Vibrations and Wave propagation," *AIAA Journal*, Vol. 27, No. 7, 1989, pp. 935–946.

[6] Yu, W., Volovoi, V. V., Hodges, D. H., and Hong, X., "Validation of the variational asymptotic beam sectional analysis (VABS)," *AIAA Journal*, Vol. 40, 2002, pp. 2105–2113.

[7] Yu, W. and Hodges, D. H., "Elasticity Solutions Versus Asymptotic Sectional Analysis of Homogeneous, Isotropic, Prismatic Beams," *Journal of Applied Mechanics*, Vol. 71, 2004, pp. 15–23.

[8] Carrera, E. and Giunta, G., "Refined beam theories based on Carrera's Unified Formulation," *International Journal of Applied Mechanics*, Vol. 2, No. 1, 2010, pp. 117–143.

[9] Carrera, E., Giunta, G., Nali, P., and Petrolo, M., "Refined beam elements with arbitrary cross-section geometries," *Computers and Structures*, Vol. 88, No. 5–6, 2010, pp. 283–293, DOI: 10.1016/j.compstruc.2009.11.002.

[10] Carrera, E., Petrolo, M., and Nali, P., "Unified formulation applied to free vibrations finite element analysis of beams with arbitrary section," *Shock and Vibrations*, 2010, DOI: 10.3233/SAV-2010-0528.

[11] Carrera, E. and Petrolo, M., "On the Effectiveness of Higher-Order Terms in Refined Beam Theories," *Journal of Applied Mechanics*, Vol. 78, 2011, doi: 10.1115/1.4002207.

[12] Carrera, E., Petrolo, M., and Varello, A., "Advanced Beam Formulations for Free Vibration Analysis of Conventional and Joined Wings," *Journal of Aerospace Engineering*, 2011, In Press.

[13] Carrera, E., Petrolo, M., and Zappino, E., "Performance of CUF approach to analyze the structural behavior of slender bodies," *Journal of Structural Engineering*, 2011, In Press.

[14] Carrera, E. and Petrolo, M., "A Beam Formulation with Shell Capabilities," *AIAA-2010-3021 51st AIAA/ASME/ASCE/AHS/ASC Structures, Structural Dynamics, and Materials Conference 18th AIAA/ASME/AHS Adaptive Structures Conference 12th, Orlando, Florida, Apr. 12-15, 2010*, 2010.

[15] Carrera, E., Giunta, G., and Petrolo, M., *Developments and Applications in Computational Structures Technology*, chap. A Modern and Compact Way to Formulate Classical and Advanced Beam Theories, Saxe-Coburg Publications, 2010.

[16] Carrera, E., Giunta, G., and Petrolo, M., *Beam Structures: Classical and Advanced Theories*, John Wiley & Sons, In Press.

[17] Carrera, E., "Theories and finite elements for multilayered, anisotropic, composite plates and shells," *Archives of Computational Methods in Engineering*, Vol. 9, No. 2, 2002, pp. 87–140.

[18] Carrera, E., "Theories and finite elements for multilayered plates and shells: a unified compact formulation with numerical assessment and benchmarking," *Archives of Computational Methods in Engineering*, Vol. 10, No. 3, 2003, pp. 216–296.

[19] Carrera, E. and Petrolo, M., "Refined Beam Elements with only Displacement Variables and Plate/Shell Capabilities," Submitted.

[20] Bathe, K., *Finite element procedure*, Prentice hall, 1996.

[21] *www.mul2.com*.

Downloaded by UNIVERSITY OF MICHIGAN on March 7, 2014 | http://arc.aiaa.org | DOI: 10.2514/6.2011-2168